Long-term performance evaluation for deep borehole heat exchanger array under different soil thermal properties and system layouts

Wanlong Cai[a], Fenghao Wang[a,*], Chaofan Chen[b], Shuang Chen[b], Jun Liu[a,c], Zhanli Ren[d], Haibing Shao[b,**]

[a]*School of Human Settlements and Civil engineering, Xi'an Jiaotong University, Xi'an, Shaanxi 710049, China*
[b]*Helmholtz Centre for Environmental Research-UFZ, Permoserstraße 15, 04318 Leipzig, Germany*
[c]*Key Laboratory of Coal Resources Exploration and Comprehensive Utilization, Ministry of Natural Resources, Xi'an, Shaanxi 710021, China*
[d]*Department of Geology, Northwest University, Xi'an, Shaanxi 710069, China*

Abstract

To meet the prospect of carbon neutrality, Deep borehole heat exchanger (DBHE) shows good potentiality in extracting deep geothermal energy for building heating, especially in densely populated urban areas of northern China. To investigate the influence on different soil thermal properties and system layouts of the DBHE array, a comprehensive numerical model has been established by OpenGeoSys software coupled TESPy toolkit and a series of scenarios are simulated. Results show that thermal conductivity lay a more important influence on heat extraction performance for DBHE array, rather than volumetric heat capacity. The thermal plume of DBHE array will grow larger along with higher thermal diffusivity. For typical geological parameters in Xi'an, the inter-borehole spacing should not be set below 15 m or it will bring a risk of freeze in circulation. The heat extraction performance and long-term sustainability of single-line layout are obviously better than other layout patterns, also with a smaller ground area needed to deploy the boreholes. This study implies that soil thermal conductivity

*Corresponding author
**Corresponding author
Email addresses: `cwl828@stu.xjtu.edu.cn` (Wanlong Cai), `fhwang@mail.xjtu.edu.cn` (Fenghao Wang), `chaofan.chen@ufz.de` (Chaofan Chen), `shuang.chen@ufz.de` (Shuang Chen), `power20113543@stu.xjtu.edu.cn` (Jun Liu), `renzhanl@nwu.edu.cn` (Zhanli Ren), `haibing.shao@ufz.de` (Haibing Shao)

is the core factor in determining the heat extraction performance of DBHE array and also gives suggestions for the system design of DBHE array in the aspect of borehole spacing and system arrangement.

Keywords: Deep borehole heat exchanger array, Heating system, Soil thermal property, System layout, Long-term sustainability

---

Nomenclature

Roman letters

C	circumference of the DBHE array (m)
c	specific heat capacity ($\mathrm{J\,kg^{-1}\,K^{-1}}$)
D_e	equivalent diameter of the pipe (m)
D_s	inter-borehole spacing in DBHE array (m)
H	heat sink/source term ($\mathrm{W\,m^{-3}}$)
h	enthalpy of circulation fluid ($\mathrm{J\,kg^{-1}}$)
$\mathbf{I}$	identity matrix (-)
k_s	roughness of pipe (mm)
L	length of pipe (m)
$\dot{m}$	mass flow of circulation fluid (kg)
M	integer (-)
N	integer (-)
P	power (W)
p	hydraulic pressure loss in the pipe network (W)
Q	heat (W)
q_n	heat flux ($\mathrm{W\,m^{-2}}$)
Re	Reynolds number (-)

S	area of the DBHE array (m^2)
T	temperature (°C)
t	time (s)
$\mathbf{v}$	vector of flow velocity ($\mathrm{m\,s^{-1}}$)
x	mass fraction of circulation fluid (-)

Greek Letters

α	thermal diffusivity ($\mathrm{m^2\,h^{-1}}$)
β_L	longitudinal heat dispersivity (m)
$\mathit{\Gamma}$	boundary
λ	thermal conductivity ($\mathrm{W\,m^{-1}\,K^{-1}}$)
$\mathit{\Lambda}$	thermal hydrodynamic dispersion tensor($\mathrm{W\,m^{-1}\,K^{-1}}$)
$\mathit{\Phi}$	heat transfer coefficient ($\mathrm{W\,m^{-2}\,K^{-1}}$)
ρ	density ($\mathrm{kg\,m^{-3}}$)
Θ	Darcy friction factor (-)

Operators

Δ	difference operator
∇	nabla vector operator
$\sum$	integral operator

Subscripts

f	circulation fluid in borehole
fl	circulation fluid in pipe network
g	grout
i	inner pipe (outflow)
in	inlet

max	maximum
o	outer pipe (inflow)
out	outlet
s	soil/rock

Abbreviations

DBHE	Deep Borehole Heat Exchanger
FEM	Finite Element Method
GSHP	Ground Source Heat Pump
TC	Thermal conductivity
TD	Thermal diffusivity
VHC	Volumetric heat capacity

1. Introduction

In recent years, countries across the world are consistently investing in energy technology and developing highly efficient, de-carbonized and renewable solution [1, 2]. At the beginning of 2021, China has also made the decision to aggressively pursue the transition towards renewable energy, trying to reach the peak carbon emission in 2030 and to achieve carbon neutrality in 2060 [3]. Compared to other renewable energy sources, geothermal energy draws more attention in recent years because of its versatile usage, stable performance and wide availability [4, 5].

Globally, the building energy consumption accounts for over 30 % of the total energy usage [6]. Within the buildings, heating and domestic hot water take a large share of more than 40 % [7] in China and 75 % in Europe respectively [8]. In the last decade, the conventional shallow borehole heat exchanger (BHE) coupled Ground Source Heat Pump (GSHP) has been widely applied for building heating and cooling in large amounts of projects [9]. In China, the application of shallow GSHP system is constrained due to its requirement on large drilling area [10] and annually unbalanced soil thermal load [11]. In comparison, geothermal heating using Deep Borehole Heat Exchanger (DBHE) [12] is being quickly accepted by the market. The pioneering attempt of DBHE can be traced back to the end of the last century, related projects have been reported in Hawaii [13] and Weissbad [14]. By prolonging coaxial pipe installed in the borehole to 2000 m∼3000 m depth, Deep Borehole Heat Exchanger (DBHE) is proposed to serve for extracting geothermal energy for building heating [15, 16]. Although the DBHE heating system has good performance and obvious benefits, only limited pilot applications exist in Europe due to its high initial drilling cost and lack of economic feasibility [17].

As the Chinese government is strongly encouraging renewable energy sources for newly constructed building heating projects, GSHP system coupled with DBHE is widely spreading in northern China. This technology is very popular in densely populated urban areas, where building thermal load is concentrated and land area is limited. There are a few DBHE coupled GSHP pilot-projects and related field tests reported in recent years, most of which are located in Xi'an city, Shaanxi province [18, 19, 20]. Based on a series of experimental tests executed by Deng et al [21], the results indicated that the average system Coefficient of Performance (COP) of DBHE coupled GSHP system can reach 4.58, which has a clear advantage over air-source or shallow ground-source heat pump systems. To further investigate the heat extraction performance and optimization of the system, considerable research on the DBHE topic has been carried out in the last few years. For example, several calculation methods have been developed by researchers for simulating the performance of DBHE, including analytical [22, 23] and numerical approaches, such as Finite Volume [24] and Finite Difference[25] methods. Modeling software based on Finite Element Method, including FEFLOW[26], FLUENT[27] and COMSOL[28]) are also widely applied to simulate the coupled thermal-hydraulic process within and surrounding the DBHE. A series of detailed numerical investigations executed by Kong et al. [29] on the heat extraction performance and system efficiency of the DBHE heating system suggests that the sustainable specific heat extraction rate should be set no more than 150 W/m. Beier [30] proposed a novelty analytical method to calculate the heat transfer performance of DBHE by applying the Laplace transform and Stehfest numerical inversion. Their results proved that the existing geothermal gradient makes a difference in the heat extraction of the DBHE. Liu et al. [31] discussed the effects of geological parameters on the thermal performance of DBHE and pointed out that thermal conductivity is the core factor for determining the heat extraction capacity of DBHE. As for the long-term sustainability of DBHE, there are also several related studies reported, focusing on the soil temperature distribution [32], intermittent heating mode [33] and heat pump performance [34] of the DBHE heating system.

It should be noticed that most of the related research of DBHE mainly concentrates on a single borehole, while the real-world projects are typically equipped with multiple boreholes or even a borehole array [18, 19]. Also, there has already been plenty of research reported in shallow GSHP systems, where the long-term performance [35], and thermal interaction analysis [36] are investigated in detail. Taking the thermal interaction and the pipe network features into consideration, research shows that the thermal performance of the BHE array will not be identical to the single BHE [37]. Corresponding optimization method has also been proposed by Bayer et al. [38]. Moreover, the state-of-art knowledge suggests that unbalanced thermal load will lead to elevated or suppressed temperature zones in the subsurface. Series of research have shown that knowing the soil temperature field and its variation is essentially necessary for the performance forecast of geothermal applications [39, 40]. In this context, the investigations on heat extraction performance and sustainability of DBHE array based on 3D comprehensive simulations, considering the thermal interaction and soil temperature variation among all the multiple boreholes, are significant for its design procedure.

In our previous work published recently [41], a numerical model established by OpenGeoSys (OGS) software and Python toolkit TESPy was developed for simulating the DBHE array. The model was validated against experimental data measured from a pilot project in Xi'an, Shaanxi Province. In that study, the discrepancy of heat extraction performance between single and multiple DBHE is clearly illustrated, while detailed analysis on performance evaluation under different system parameters has not been carried out. In this context, several scientific questions remain for the DBHE array system: Will the heat extraction performance of the DBHE array show an obvious difference under different soil thermal properties? After the thermal interaction among DBHEs is taken into consideration, which soil thermal-physical parameter has the dominant influence on the system performance? How does the system layout of the DBHE array affect its long-term sustainability?

In this paper, the above scientific questions were investigated by a set of elaborated numerical simulations. A DBHE array model was constructed by OpenGeoSys-TESPy software and deployed based on the actual geological parameters in Xi'an, China. Through the numerical simulations, the variation of heat extraction performance and soil temperature field were analyzed in detail. Then, long-term simulations were carried out and the heat extraction performance of the DBHE array under different soil thermal properties was evaluated. At the next step, the sustainability of the DBHE array under several array layouts was also investigated, the effect of inter-borehole spacing and the impact of array geometry were also discussed. In the end of the manuscript, practical and instructive suggestions are made to improve the design procedure of DBHE heating systems.

2. Methodology

In this section, the model framework and numerical approach applied for the simulation of DBHE array are introduced.

2.1. Dual-continuum FEM approach

In the present model framework for DBHE simulation, many researchers select different numerical approaches, since they are more capable of handling the flexible initial and boundary conditions that emerge from the field study. Specifically, the two-dimensional (2D) axial-symmetric domain is widely chosen because of its simplicity and potential in saving computational resources, including the research proposed by Li et al. [27] and Bu et al. [42]. However, when investigating the thermal interaction among multiple DBHEs, 2D axial-symmetric domains are no longer sufficient. Especially when the subsurface stratification and different thermal characteristics of the layers are considered, a fully discretized 3D domain has to be constructed with multiple DBHEs explicitly depicted in it. When the kilometer-long borehole is discretized with millimeter-wise details, the resulting size of the mesh often exceeds the capacity of the latest high-performance-computing platforms.

In the field of deep coaxial borehole heat exchangers simulation, the coaxial pipe with an annular inlet (CXA) is recommended for heat extraction [43]. The governing equations for the fluid inside the centered and annular borehole are given by

$$\rho_f c_f \frac{\partial T_i}{\partial t} + \rho_f c_f \mathbf{v}_i \cdot \nabla T_i = \nabla \cdot (\mathit{\Lambda}_i \cdot \nabla T_i) + H_i \tag{1}$$

$$\text{with the Robin type of BC :}$$

$$q_{nT_i} = -\mathit{\Phi}_{io} \left(T_o - T_i\right) \ \text{ on } \mathit{\Gamma}_i \tag{2}$$

$$\rho_f c_f \frac{\partial T_o}{\partial t} + \rho_f c_f \mathbf{v}_o \cdot \nabla T_o = \nabla \cdot (\mathit{\Lambda}_o \cdot \nabla T_o) + H_o \tag{3}$$

$$\text{with the Robin type of BC :}$$

$$q_{nT_o} = -\mathit{\Phi}_{io} \left(T_i - T_o\right) - \mathit{\Phi}_{og} \left(T_g - T_o\right) \ \text{ on } \mathit{\Gamma}_o \tag{4}$$

where ρ_f, c_f refer to the density and specific heat capacity of the circulation fluid. The $\mathbf{v}$ and Λ denote the flow velocity and thermal hydrodynamic dispersion tensor of fluid in the borehole, respectively. The H and Γ are the heat sink/source term and heat transfer boundary. Φ_{io} refer to the thermal resistance between inner and outer pipe while Φ_{og} denote the thermal resistance between outer pipe and grout [44].

The term of hydrodynamic thermal dispersion tensor is defined as

$$\Lambda_f = (\lambda_f + \rho_f c_f \beta_L \|\mathbf{v}_f\|)\,\mathbf{I} \tag{5}$$

where β_L denote the longitudinal heat dispersivity and $\mathbf{I}$ refer to the identity matrix.

Also, the governing equations for the grout surrounding the outer pipe and the soil surrounding the borehole are given by

$$\rho_g c_g \frac{\partial T_g}{\partial t} = \nabla \cdot (\lambda_g \cdot \nabla T_g) + H_g \tag{6}$$

with the Robin type of BC :

$$q_{nT_g} = -\Phi_{og}\,(T_o - T_g) - \Phi_{gs}\,(T_s - T_g) \;\text{ on } \Gamma_g \tag{7}$$

$$\rho_s c_s \frac{\partial T_s}{\partial t} = \nabla \cdot (\Lambda_s \cdot \nabla T_s) + H_s \tag{8}$$

with the Robin type of BC :

$$q_{nT_s} = -\Phi_{gs}\,(T_g - T_s) \;\text{ on } \Gamma_s \tag{9}$$

in which the detailed calculation of thermal resistance Φ between soil/grout and borehole can also be found in Diersch et al. [44].

The Dual Continuum Finite Element Method (DC-FEM) is adopted and implemented [45] in the open-source software OpenGeoSys (OGS) [46], in which the implemented numerical framework is slightly different than those as in COMSOL or FLUENT software. Following the DC-FEM approach, the simulation domain can be divided into two compartments, while governing equations are respectively imposed on 1D line elements for the boreholes and 3D prism elements for the surrounding subsurface. The heat flux between each borehole and the surrounding subsurface, which is determined by the temperature difference between these two compartments, is set as the Neumann-type of boundary conditions in the simulation. Through the adoption of the Dual Continuum approach, the number of nodes in the model domain will be significantly reduced while the flexibility of model configuration can still be maintained. The detailed discretized approach can be found in the publication of Al-Khoury et al. [47] and Diersch et al[44, 48]. Therefore, the calculation cost for the long-term simulation of the DBHE array becomes acceptable. More detailed documentation on benchmarks and tutorials of DBHE modeling features can be found on the official website of OpenGeoSys [49].

2.2. OpenGeoSys-TESPy coupling

Since the DBHE array is connected through a pipe network in real-world projects, the outflow from each DBHE borehole will mix in the manifolds and then send to the heat pump (see Fig. 1). After exchanging heat there, a circulation pump will re-distribute the ground-loop fluid back to each borehole located in different places. In order to reflect the real configuration of fluid circulation in the DBHE array system, the conventional boundary conditions which set the constant inflow temperature or transient thermal load of each borehole need to be changed to reflect the hydro-thermal processes in the connecting pipe network. The Thermal Engineering Systems in Python (TESPy) toolkit is an open-source Python library developed by Witte and Tuschy [50]. It is adopted here to simulate the hydraulic-thermal characters of the pipe network. With predefined characteristics of each component, the pressure, temperature and enthalpy at each junction of the pipe network can be calculated with TESPy. The mass and enthalpy balance is given by the following equations [50]:

$$\sum_{M} \dot{m}_{in,M} \cdot x_{fl,in,M} = \sum_{N} \dot{m}_{out,N} \cdot x_{fl,out,N} \tag{10}$$

$$\sum_{M} \dot{m}_{in,M} \cdot h_{in,M} = \sum_{N} \dot{m}_{out,N} \cdot h_{out,N} + P + \dot{Q} \tag{11}$$

where the $\dot{m}$, x and h are mass flow, mass fraction and enthalpy of every connection. Then the values of P and $\dot{Q}$ are deduced by the variation of power and heat for every individual components.

The Darcy-Weisbach equation is adopted to calculate the hydraulic pressure drop in the pipe network, which is given by

$$p_{in} = p_{out} + \frac{\rho_f \cdot v_f^2 \cdot \Theta\left(\mathrm{Re}, k_s, D_e\right) \cdot L}{2 \cdot D_e} \tag{12}$$

where the p_{in} and p_{out} are the pressure at the inlet and outlet of pipe respectively. The ρ_f and v_f are the density and flow velocity of the fluid. The Darcy friction factor Θ is calculated by several parameters, in which the Reynolds number Re is defined by flow rate, characteristic length and kinematic viscosity, k_s refers to the roughness of pipe, and the D_e is the equivalent diameter of the pipe. The L is the length of pipe.

For the comprehensive simulation of DBHE array and the connecting building loop, TESPy version 0.3.2 and OpenGeoSys 6.3.2 are coupled together by using Python library Pybind11. The technical detail of the OpenGeoSys-TESPy can be found in Chen et al. [37].

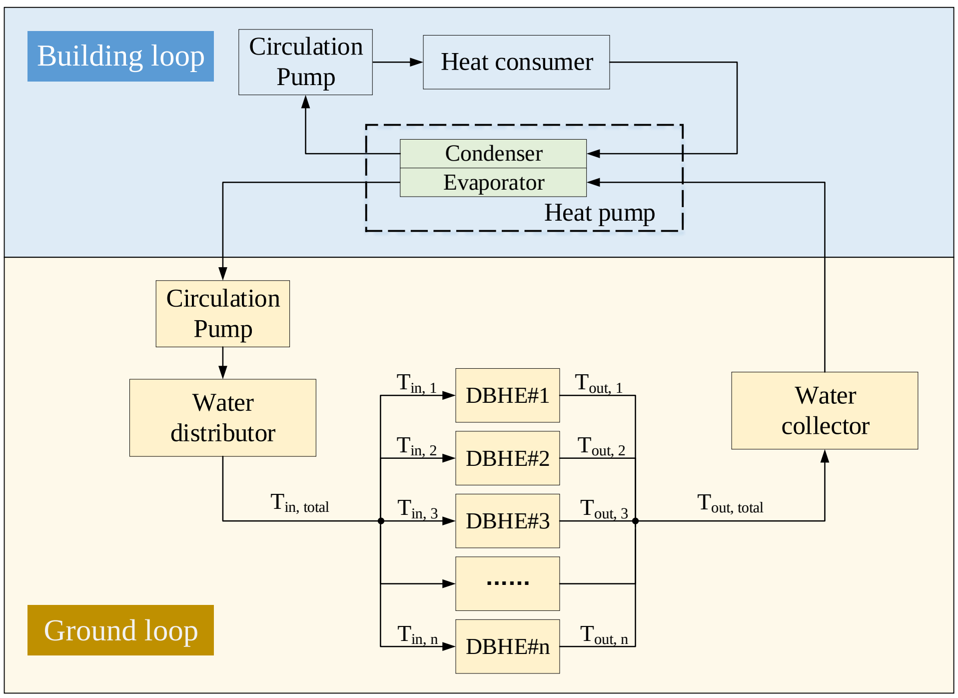

Figure 1: Schematic diagram for calculating logic of OpenGeoSys-TESPy coupling solution

2.3. Model verification

The DBHE array model implemented in OpenGeoSys software has previously been verified against analytical solution [37, 51]. The same feature has already been applied in real-world projects and its results have been validated by monitoring data from actual GSHP projects in Cologne [52] and Leicester [53]. As for the deep geothermal application in China, thorough model validation was conducted based on a 5-DBHE pilot project in Xi'an city [41]. The model was capable of reproducing the evolution of circulation temperature over an entire heating season. The model predicted temperature profile, in comparison to the monitored data, is illustrated in Fig. 2. As shown in this comparison, the maximum relative difference between monitored and simulated values is no more than 1.1 °C (less than 5.0 %). The results ensure that the coupled OGS-TESPy model has enough accuracy and could be used in investigating the long-term sustainability of the DBHE array.

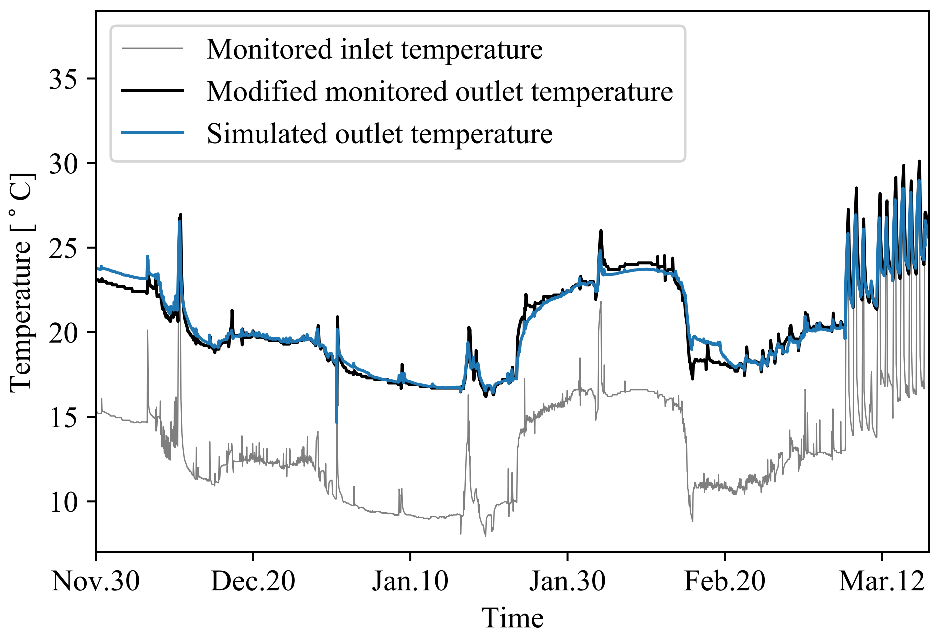

Figure 2: Verification of proposed OGS-TESPy model against in-situ monitoring data (adjusted from Cai et al. [41])

3. Model configuration

As discussed in the introduction, DBHE based geothermal heating projects have shown a rapidly growing trend in northern China. Until the end of 2020, the total floor area equipped with the DBHE heating system in Xi'an has reached 15 million m^2. Therefore, the model scenarios in this study are configured based on the subsurface characteristics for the systems located in Xi'an. All the detailed parameters of the DBHE array system are summarized in Table 1.

Table 1: Detailed parameters of the DBHE array system

Item	Parameter	Value	Unit
Borehole	Borehole depth	2500	m
	Borehole diameter	0.2159	m
	Borehole spacing	15	m
	Outer diameter of inner tube	0.1100	m
	Wall thickness of inner tube	0.0100	m
	Thermal conductivity of inner tube wall	0.42	W m^{-1} K^{-1}
	Outer diameter of outer pipe	0.1778	m
	Wall thickness of outer pipe	0.0092	m
	Thermal conductivity of outer pipe wall	40	W m^{-1} K^{-1}
	Average heating extraction rate	130	W m^{-1}
Grout	Density	2.190×10^3	kg m^{-3}
	Specific heat capacity	1.735×10^3	J Kg^{-1} K^{-1}
	Thermal conductivity	1.2	W m^{-1} K^{-1}
Circulating fluid	Thermal conductivity	0.6	W m^{-1} K^{-1}
	Specific heat capacity	4.190×10^3	J kg^{-1} K^{-1}
	Density	998	kg m^{-3}
	Dynamic viscosity	9.310×10^{-4}	kg m^{-1} s^{-1}

At the top and bottom surface of the model domain, the average ambient air temperature of 14.8 °C and typical geothermal heat flux 60 mW/m^2 [54] of Xi'an are imposed as Dirichlet and Neumann boundary conditions respectively. The specific heat extraction rate on the DBHE is set to 130 W/m (in total 325 kW for a single 2500 m borehole), which is suggested by [29], also examined and approved by many other researchers [19]. As for the initial condition, the typical geothermal gradient in Xi'an is set as 35.0 °C/km. According to the published geological data [55] and in-situ test results from realistic projects [41], the soil thermal properties, including thermal conductivity (TC) and volumetric heat capacity (VHC), were typically set in two different levels (high or low). Based on the value of thermal diffusivity (TD), scenarios A to D are designed to represent different soil thermal properties. The model scenarios are then generated with a 2×2 combination of the soil properties (see Table 2). To investigate the difference of heat extraction performance effecting by soil thermal properties between single DBHE and DBHE array, the scenarios A to D are all imposed for both a single DBHE model and a 5-DBHE array model, while other parameters in the model follow the setting in Table 1.

Table 2: Detailed geophysical parameters in the simulated scenarios

Geological formation	Geophysical parameters[1]	Scenario.A (Higher TD)	Scenario.B (High TD)	Scenario.C (Low TD)	Scenario.D (Lower TD)
Clay (0∼500 m)	λ	2.0	1.6	2.0	1.6
	ρC_p	2.52×10^6	2.52×10^6	2.84×10^6	2.84×10^6
	α	2.85×10^{-3}	2.28×10^{-3}	2.53×10^{-3}	2.03×10^{-3}
Gravel (500∼900 m)	λ	2.1	1.63	2.1	1.63
	ρC_p	1.91×10^6	1.91×10^6	2.70×10^6	2.70×10^6
	α	3.96×10^{-3}	3.08×10^{-3}	2.80×10^{-3}	2.18×10^{-3}
Mudstone (900∼1700 m)	λ	2.3	1.7	2.3	1.7
	ρC_p	1.88×10^6	1.88×10^6	2.82×10^6	2.82×10^6
	α	4.41×10^{-3}	3.26×10^{-3}	2.84×10^{-3}	2.17×10^{-3}
Sandstone (> 1700 m)	λ	2.5	1.81	2.5	1.81
	ρC_p	1.96×10^6	1.96×10^6	2.97×10^6	2.97×10^6
	α	4.59×10^{-3}	3.32×10^{-3}	3.03×10^{-3}	2.19×10^{-3}

[1] λ denotes the thermal conductivity ($\mathrm{Wm^{-1}K^{-1}}$); ρC_p is the volumetric heat capacity ($\mathrm{Jm^{-3}K^{-1}}$); α is the thermal diffusivity ($\mathrm{m^2/h}$).

In order to prevent the thermal plume from interfering with the domain boundary, the domain size is set to be 300 × 300 × 2700 m. The total mesh nodes and elements number then account for 90,446 and 174,028, respectively. Based on our previous work [41], the time step size of the simulation is first chosen to be 1 h in the heating season and later increased to 6 h during the recovery period, so that the overall calculation time can be reduced. This time step size has been confirmed also by other researchers' work [23] to be small enough to maintain the accuracy of the simulation results. The aforementioned simulation scenarios A to D are all run for 15 years, which is the typical life-cycle span of an HVAC system in China [56].

4. Numerical results

In this section, the impact of different soil thermal properties on the long-term heat extraction performance of both single and multi-DBHE systems is investigated. Moreover, the sustainability of the DBHE array system under different system layouts is also evaluated.

4.1. Soil thermal properties

Fig. 3 illustrates the development of ground-loop circulation temperature in both the single and multiple DBHE systems, under the influence of different soil thermal properties. According to Fig. 3(a), the simulation results show that the circulation temperatures for single DBHE with low thermal diffusivity (Scenario C) and higher thermal diffusivity (Scenario A) are distinctly higher than the other two scenarios. With the volumetric heat capacity kept the same, the inlet temperature of the single DBHE in the low TD case (Scenario C) is 8.88 °C higher than the lower TD case (Scenario D) at the end of the 15th year. Considering the thermal conductivity in the higher (Scenario A) and low TD (Scenario C) are the same, the circulation temperature difference is just 1.27 °C at the end of the 15th year. This illustrates that the volumetric heat capacity has only a minor influence on the heat extraction performance of the single DBHE system, while the thermal conductivity has a greater impact on the long-term heat extraction. As for the multi-DBHE array, similar results can be seen in Fig. 3(b) for the four scenarios. It is clearly observed that, along with the increasing time, the heat extraction performance of the DBHE array shows a decreasing trend in comparison to the single DBHE cases. The reason behind this trend is the presence of thermal interaction among the boreholes and the resulting cold accumulation in the subsurface. For the different thermal conductivity, the circulation temperature of the array in a high-level TC scenario (e.g. Scenario C) is 9.12 °C higher than the low TC case (e.g. Scenario D). With different volumetric heat capacities (Scenario A and C), the circulation temperature difference between the two scenarios extended to 2.25 °C, suggesting that the impact of volumetric heat capacity on heat extraction performance of DBHE array is more intense than for single DBHE. This can be explained by more severe cold accumulation among the multiple array induced by lower volumetric heat capacity or higher thermal diffusivity. Overall, it can be seen that the volumetric heat capacity has a minor impact on heat extraction performance for both single and multi-DBHE systems. In comparison, the thermal conductivity of the surrounding soil has a much larger impact on the long-term performance.

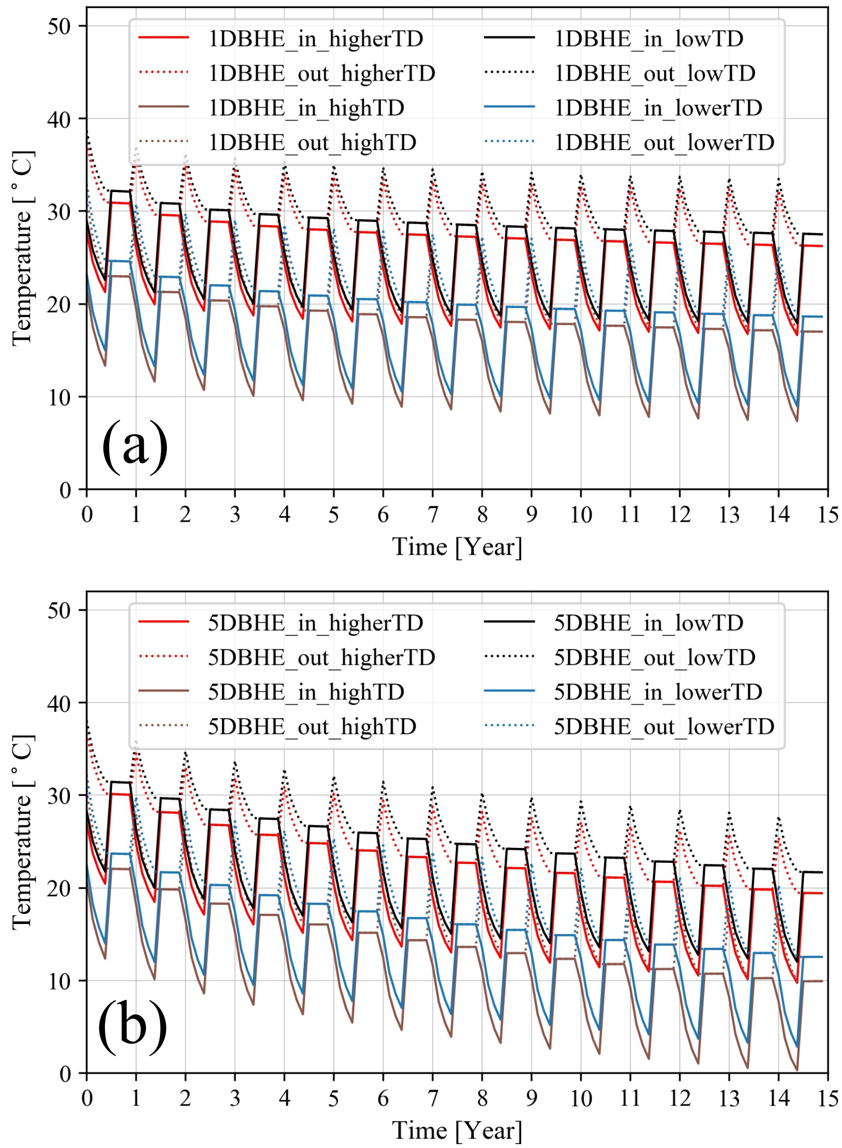

Figure 3: Overall inlet and outlet temperature of single DBHE (a), and DBHE array (b) under different soil thermal properties

Fig. 4 compares the maximum outlet temperature difference (between the DBHE located in the center and edge of the field with four different scenarios). By adopting the pipe network concept to mimic the realistic connection in DBHE array heating system, the inlet temperatures for each DBHE are kept the same. Then the outlet temperature will differ from one DBHE to another, influenced by the varying soil temperatures at different locations of the subsurface. Therefore, with a larger outlet temperature difference in a DBHE array, it illustrates that there exists a more severe draw-down of soil temperature in the surrounding subsurface, or even a distinct cold accumulation at the center of the DBHE array after long-term operation. Results show that this temperature difference in multiple DBHE array increases with the increasing thermal diffusivity, which means the thermal interaction in the DBHE array is more intense with higher thermal diffusivity. With an average value of thermal diffusivity of 4.08×10^{-3}, 3.05×10^{-3}, 2.83×10^{-3} and 2.15×10^{-3} $\mathrm{m}^2\,\mathrm{h}^{-1}$ for Scenario A to D, the maximum outlet temperature difference in DBHE array raises from 0.62 °C to 0.74 °C at the end of 15th year. This also confirms that the load shifting behaviors caused by pipe network features in the DBHE array are quite limited, which is proposed in our previous work [41].

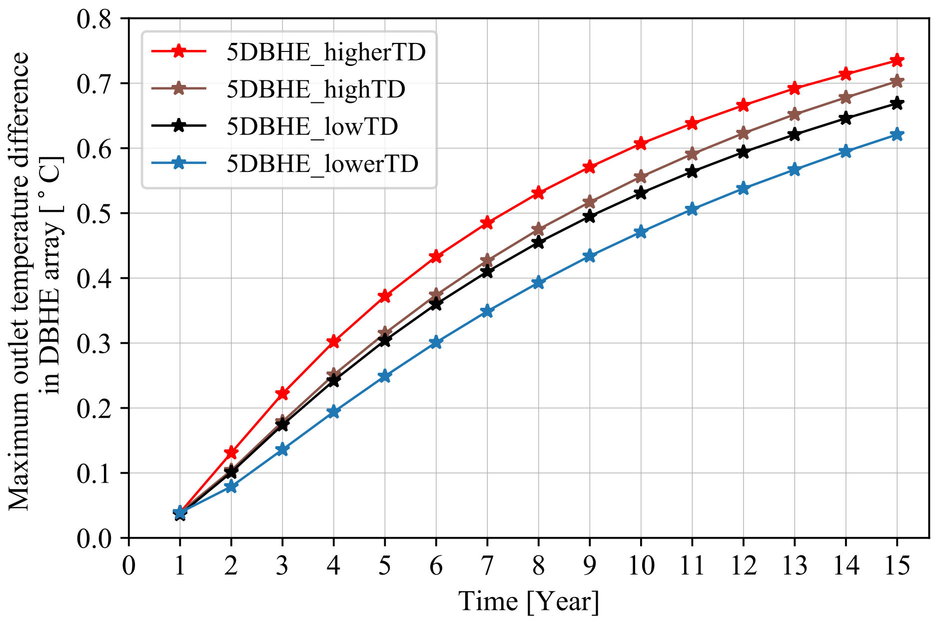

Figure 4: Maximum Outlet temperature difference among individual DBHEs within the DBHE array under four different thermal diffusivities

Fig. 5 and Fig. 6 depict the soil temperature distributions at 2300 m depth for single and multiple DBHE array under four different scenarios of soil thermal properties. Fig. 5 shows that single DBHE suffers an obvious cold accumulation over the long-term operation. With high-level TC (Fig. 5(b)), the soil temperature drop is less than the low-level TC (Fig. 5(a)), which indicates better long-term sustainability. As for high-level VHC (Fig. 5(b)), the soil temperature drop is almost the same (only 0.11 °C difference) as the low-level VHC (Fig. 5(d)), while the radius of the thermal plume in the low VHC scenario is much larger than the high VHC case. It can be seen that, with higher thermal diffusivity (higher thermal conductivity and lower volumetric heat capacity), the radius of the thermal plume from a single DBHE tends to extend further.

For the DBHE array, Fig. 6 reveals the same trend as in Fig. 5, in which a higher thermal conductivity brings a smaller soil temperature drop and better sustainability for DBHE array in long-term heat extraction. It should be noticed that, except for the larger draw-down in soil temperature caused by cold accumulation in the DBHE array, the minimum soil temperature for low-level VHC (Fig. 6(d)) is 1.64 °C less than the high-level VHC (Fig. 6(b)), which is more obvious than single DBHE. This means for DBHE array a lower volumetric heat capacity (or higher thermal diffusivity) will introduce more severe thermal interaction among multiple DBHEs and trigger severe cold accumulation.

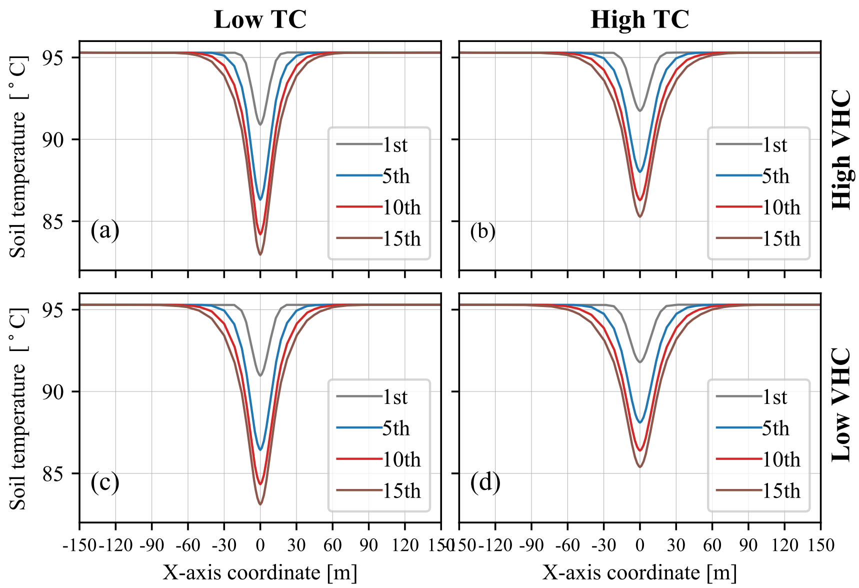

Figure 5: Soil temperature distribution of single DBHE under four different scenarios for soil thermal properties

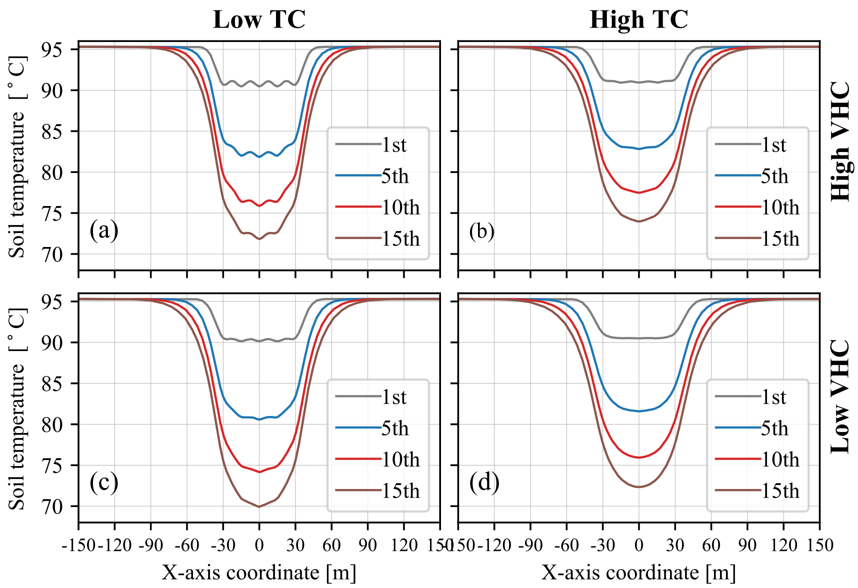

Figure 6: Soil temperature distribution of DBHE array under four different scenarios for soil thermal properties

Fig. 7 and Fig. 8 illustrate the radial thermal plume distribution at 2300 m depth for the single and multiple DBHE case respectively. A difference of 0.5 °C in comparison to the initial temperature has been used to determine the boundary of the thermal plume (marked with black dash line in Fig. 7 and Fig. 8). With the thermal diffusivity value rising from an average value of 2.15×10^{-3} to 4.08×10^{-3} $\mathrm{m^2\,h^{-1}}$, the radius of the thermal plume will increase from 41.6 m to 52.5 m). In the DBHE array case, Fig. 8 shows that the thermal plume radius will also grow from 74 m, 79.4 m, 80.1 m to 87.7 m, along with the thermal diffusivity increases from 2.15×10^{-3}, 2.83×10^{-3}, 3.05×10^{-3} to 4.08×10^{-3} $\mathrm{m^2\,h^{-1}}$. These results manifest that the size of the thermal plume will expand with increasing thermal diffusivity values, while the heat extraction performance can not be foreseen only by the value of thermal diffusivity.

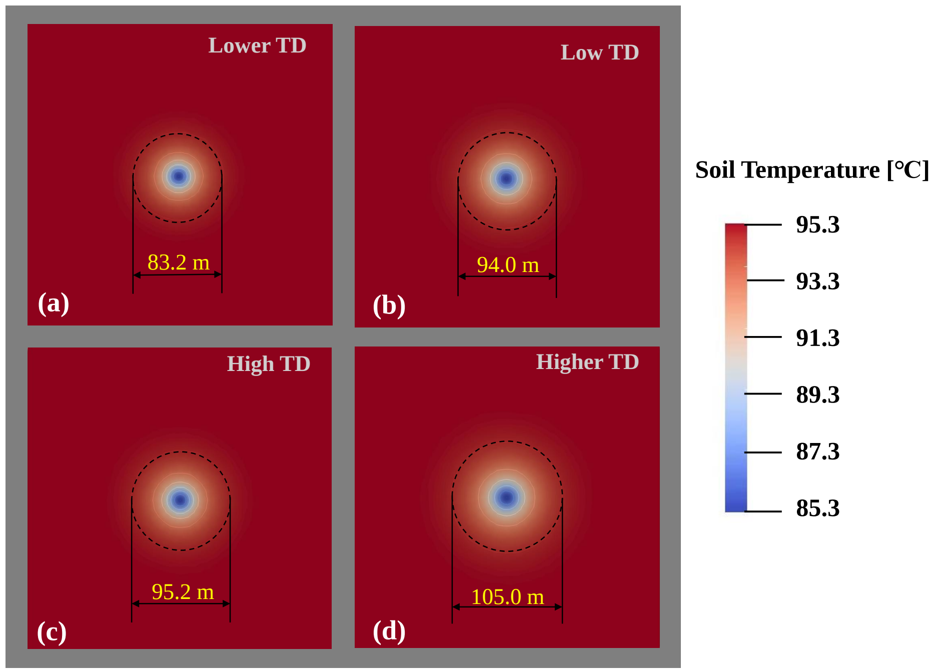

Figure 7: Thermal plumes for single DBHE under four scenarios with different soil thermal properties

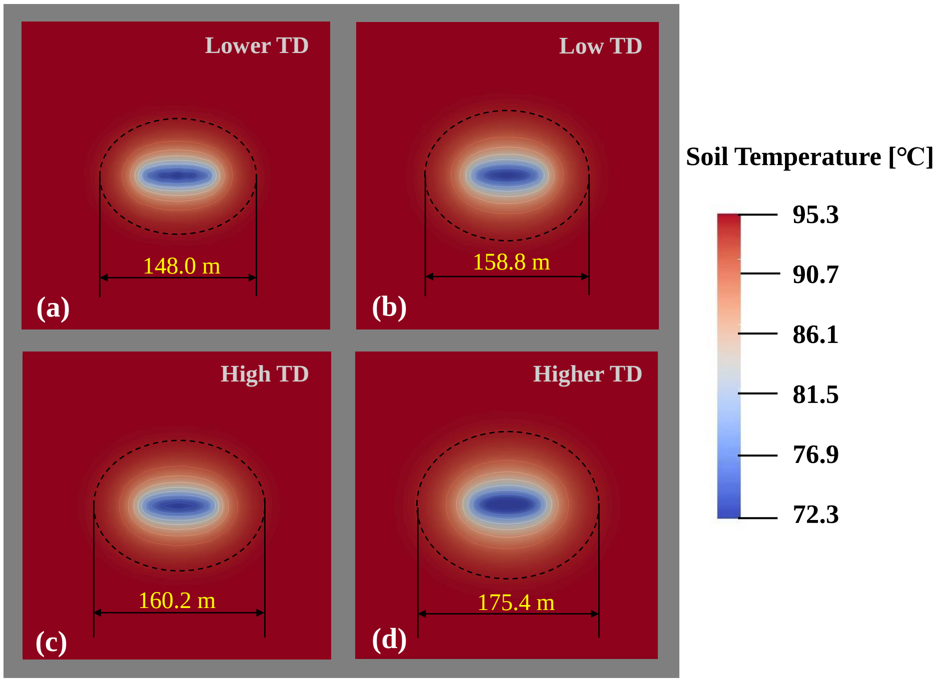

Figure 8: Thermal plumes for DBHE array under four scenarios with different soil thermal properties

4.2. Inter-borehole spacing

For a typical DBHE project located in Xi'an, the inter-borehole spacing is usually set to 15 m for the convenience of drilling. In this section, a series of simulation was conducted with the inter-borehole spacing adjusted to 10 m and 20 m. The impacts of different spacing for DBHE array on the heat extraction performance are investigated. Also, the average heat extraction rate used in evaluating the system layouts in this and the following section is adjusted to the maximum suggested value of 150 W/m [43]. The soil thermal properties of Scenario A are chosen to execute the simulation.

Fig. 9 depicts the evolution of inlet and outlet temperature of DBHE array under different inter-borehole spacing. Since water is used throughout this study as the circulation fluid, the lowest circulation temperature threshold is set to 0 °C prevent freezing in the pipe network. It could be found in Fig. 9 that, with 10 m of borehole spacing, the circulation temperature will be close to the lower limit after more than 10 years' operation, suggesting the long-term sustainability of the system may be impaired. In comparison, models with the 15 m and 20 m spacing between the boreholes show considerably better higher circulation temperature. Therefore, for typical soil thermal properties and maximum suggested thermal load, the inter-borehole spacing for the DBHE array should be set at least 15 m to ensure that the long-term stable operation can be obtained.

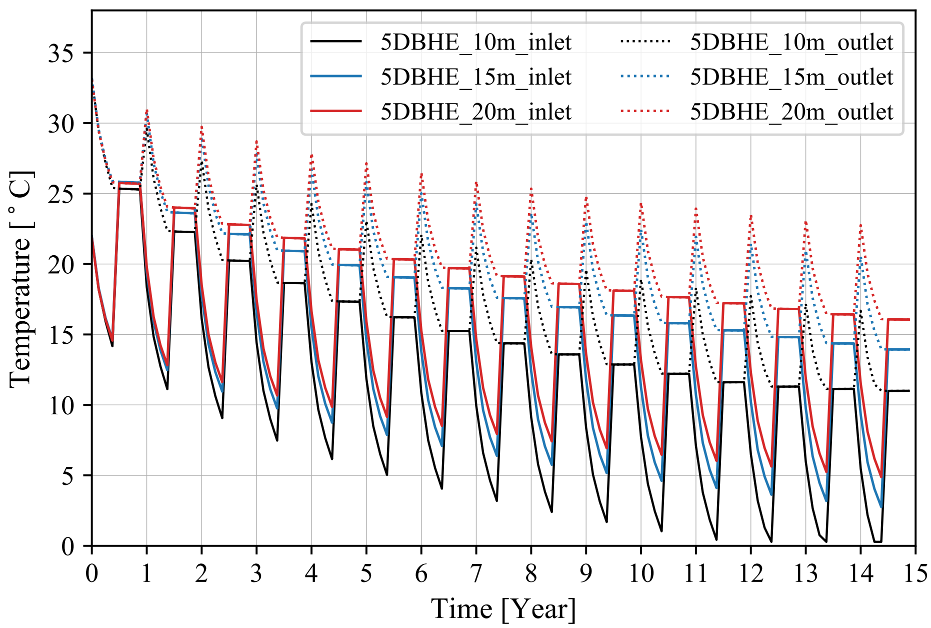

Figure 9: Overall inlet and outlet temperature of DBHE array with different borehole spacing

Diving into the details for different inter-borehole spacing scenarios, Fig. 10 illustrates that the maximum outlet temperature difference in the DBHE array has an obvious increase with a smaller inter-borehole spacing. This illustrates that the thermal interaction among multiple DBHEs will aggravate with smaller borehole spacing and more severe cold accumulation will occur at the center of the surrounding subsurface. With the 10 m spacing between the boreholes, the maximum outlet temperature difference at the end of the 15th year reaches 1.09 °C, which is almost two times larger than the 20 m borehole spacing scenario (0.60 °C of maximum outlet temperature difference).

Meanwhile, Fig. 11 also manifests that a larger inter-borehole spacing can bring more subsurface into the heat extraction process and will not suffer severe cold accumulation. For the inter-borehole spacing of 20 m, the maximum soil temperature drop after 15th years' operation is 75.11 °C. With the increase of inter-borehole spacing from 10 m to 20 m, the soil temperature drop has an obvious decrease of 10.61 °C, showing better sustainability after long-term heat extraction of DBHE array system.

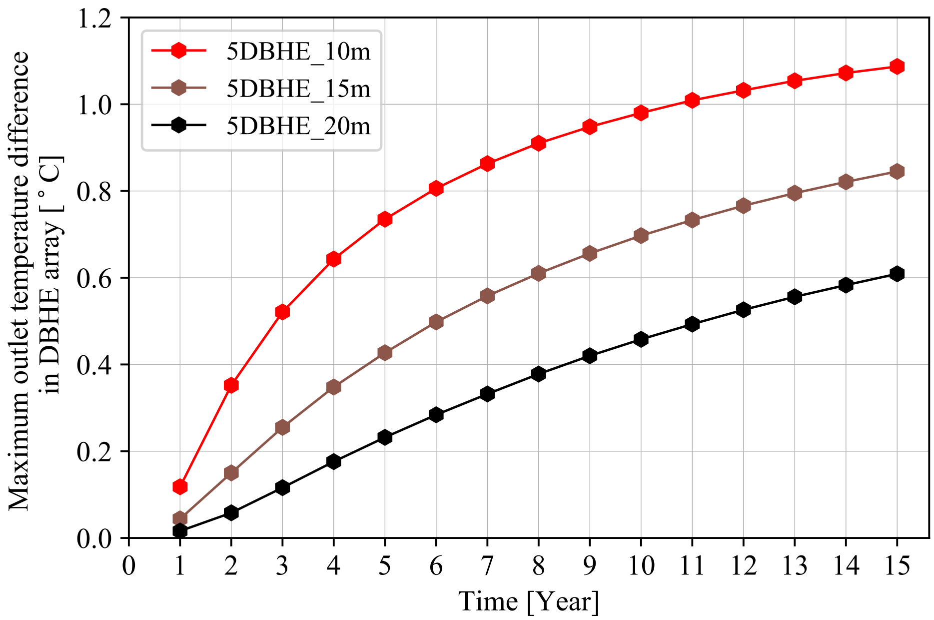

Figure 10: Maximum Outlet temperature difference among individual DBHEs within the DBHE array under different borehole spacing

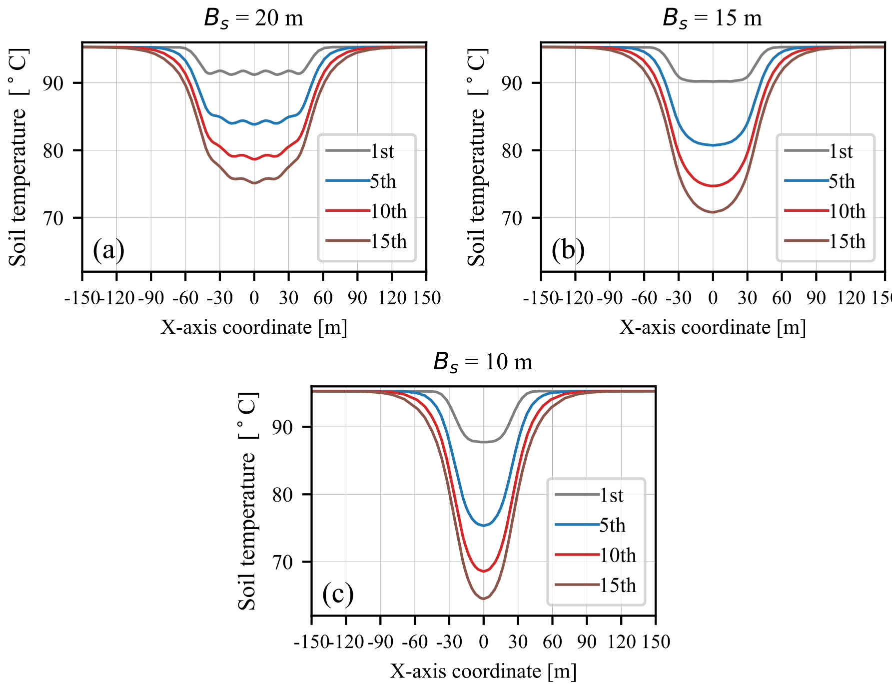

Figure 11: Soil temperature distribution of DBHE array with different borehole spacing

4.3. Arrangement geometry

For most of the DBHE projects in Xi'an, the borehole array is usually arranged in a single line layout (see Fig. 12) [41]. This is mainly because that such arrangement can fully utilize the free space between the buildings and the project land boundary. In this section, several types of arrangement geometries are proposed to investigate the potential to increase system performance or enhance its long-term sustainability.

Fig. 12 demonstrates several arrangement geometries of DBHE array, including the traditional single-line layout, circle layout (the center DBHE was removed to prevent cold accumulation), and polyline layout. The multi-row layout (e.g. 3×3 layout for 9 DBHEs) is not considered because the centered DBHE in this type of layout will suffer severe cold accumulation and will not obtain a better heat extraction performance of the whole DBHE array. The number of boreholes in the DBHE array is set as 5 for convenience and typicality of simulation. In all three arrangements, the boreholes are connected in a parallel manner, and the inter-borehole distances are all set to the same value D_s of 15 m in this study.

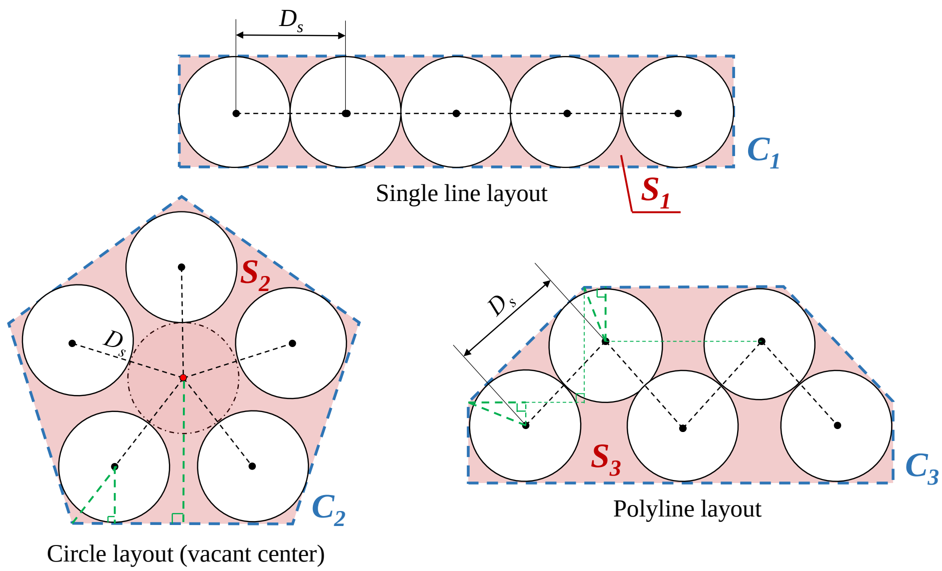

Figure 12: Diagram of three different arrangement geometry of DBHE array

The long-term simulation results could be seen in Fig. 13, after a long period of operation, the single line layout gains higher circulation temperatures than the other two layouts. At the end of the 15th year, the circulation temperature of DBHE array with the single line layout maintains over 2.76 °C, which is beyond the temperature threshold to prevent the freezing in the system. The circulation temperature drop of DBHE array with polyline layout is higher than the other two scenarios, which implies unsatisfactory sustainability in long-term operation.

Also, the thermal plume at the depth of 2300 m is shown in Fig. 14, the shape of three thermal plumes all tend to be ellipse after long-term operation. The half-length of the major axis is selected to be representative of the thermal plume radius. The results in Fig. 14 manifest that the thermal plume radius for single line layout (88.3 m) is larger than circle layout (77.1 m) and polyline layout (78.0 m), also a severe cold accumulation in the polyline layout can be observed. This manifests the single line layout could extract more heat from larger surrounding subsurface and thus obtain higher circulation temperature and also better long-term sustainability.

Except for the heat extraction performance, the ground area of DBHE array with the different arrangement also needs to be assessed. For the three arrangement geometries in Fig. 12, a group of auxiliary lines is added (green line) on the circle and polyline arrangement. The ground area can be then deduced by using geometric theorem and the Trigonometric function formula. With an inter-borehole spacing of 15 m, the ground area of DBHE array for single line, circle and polyline are respectively 1125.00 m^2, 1400.60 m^2 and 1245.78 m^2. It can be seen that the single line layout has the smallest area, while the other two layouts all need a larger ground area to deploy. The results illustrate that the single line layout should be selected as the proper arrangement geometry for the DBHE array. Because it has better sustainability in long-term heat extraction and does not need a larger space to implement.

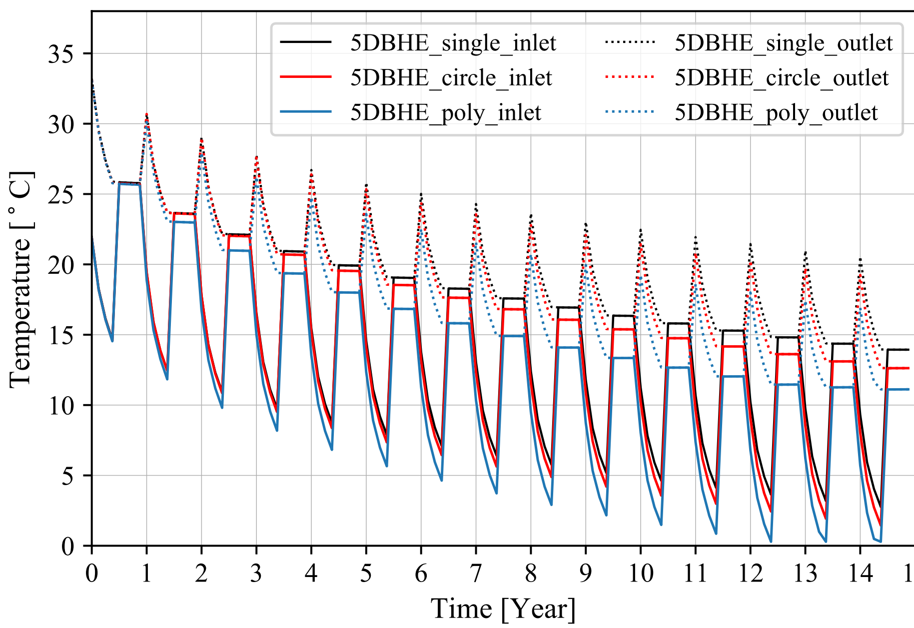

Figure 13: Overall inlet and outlet temperature of DBHE array with different system layout

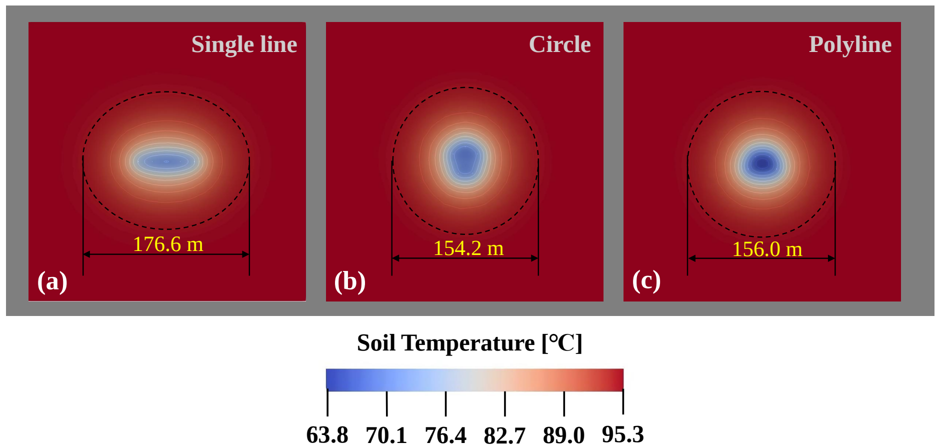

Figure 14: Thermal plumes of DBHE array with three different arrangement geometry

5. Discussion

With a typical heat extraction rate (130 W/m), Fig. 15 illustrates the soil temperature distribution and radial thermal plumes of a single DBHE after 15 years' operation. Considering the temperature difference compared to the initial soil temperature as 0.5 °C, results depict that the radius of thermal plume at the end of 15 years reaches 53.4 m. For a smaller temperature difference threshold, the value of the maximum thermal plume radius may even increase. In the aforementioned studies, results show that even an inter-borehole spacing of 20 m is enough for maintaining the long-term sustainability in the entire life span of DBHE array system. This information can be conducive to the system design of DBHE array, that is the inter-borehole spacing of DBHE array can be set as lower than the thermal plume radius. Completely avoiding the thermal interaction among DBHEs in the DBHE array may cost a huge construction area to deploy the boreholes, a certain degree of soil temperature drop caused by thermal interaction can be accepted. If the heat extraction performance and the circulation temperature variation are carefully maintained and monitored, a reasonable inter-borehole spacing can be selected to serve for long-term sustainability along with convenience in project construction.

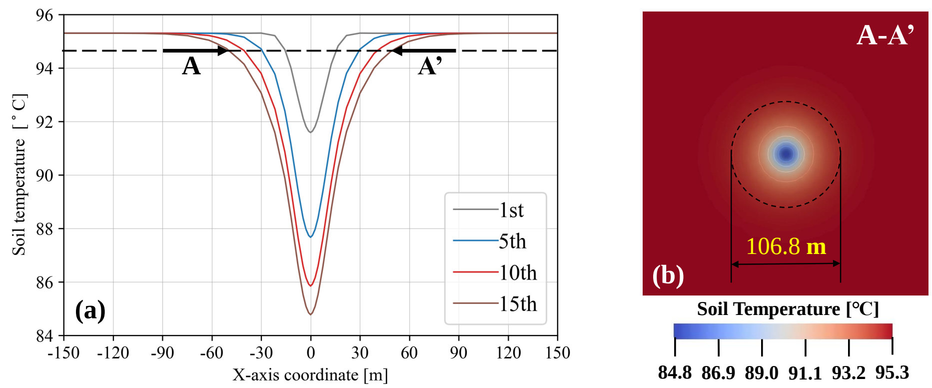

Figure 15: (a) Soil temperature distribution of single DBHE at the depth of 2300 m; (b) Thermal plumes of single DBHE after 15 years' operation

6. Conclusion

In this study, a series of numerical models are constructed to simulate the heat extraction performance and long-term sustainability of DBHE array. The typical geological formation and soil thermal properties of Xi'an, China are selected to be the parameters used in the simulation. Several scenarios are simulated and evaluated to reveal the long-term behavior and system sustainability of the DBHE array, including a set of thermal conductivity, volumetric heat capacity and thermal diffusivity, different inter-borehole spacing and arrangement geometry. In comparison, the single DBHE with the same setting is also investigated in a long-term simulation. To be more specific:

- Higher thermal conductivity and higher volumetric heat capacity will be helpful to improve the heat extraction performance of a DBHE array. Thermal conductivity has a stronger impact on heat extraction performance in both single and multiple DBHE cases. A higher level of volumetric heat capacity value will lead to stronger cold accumulation in the long term, especially for multiple DBHE arrays.

- With higher average thermal diffusivity of the subsurface, a larger thermal plume will always be produced. For DBHE array cases, the thermal plume radius will grow from 74 m to 87.7 m, along with the thermal diffusivity increases from 2.15×10^{-3} to 4.08×10^{-3} $\mathrm{m^2\,h^{-1}}$.

Nevertheless, thermal diffusivity should not be regarded as a criterion in evaluating the heat extraction performance of the DBHE array system.

- With the 10 m spacing between the boreholes, the circulation temperature will be close to 0 °C after more than 10 years' operation. Also, the DBHE array will suffer more severe cold accumulation with smaller borehole spacing. For typical geological parameters in Xi'an, the inter-borehole spacing should be at least 15 m, otherwise, it has a risk of freezing in pipelines.

- The single line layout is the preferred arrangement geometry of the DBHE array. Although its thermal plume radius is larger, the heat extraction performance and long-term sustainability in the single-line layout are better than other types of arrangement. Also, the single line layout needs a smaller ground area to deploy the boreholes, which is more accepted in project construction.

CRediT authorship contribution statement

Wanlong Cai: Conceptualization, Methodology, Software, Validation, Writing - Original Draft, Visualization. **Fenghao Wang:** Conceptualization, Formal analysis, Project administration, Funding acquisition. **Chaofan Chen:** Methodology, Software, Investigation, Writing - Review & Editing. **Shuang Chen:** Methodology, Software, Writing - Review & Editing. **Jun Liu:** Validation, Formal analysis, Investigation. **Zhanli Ren:** Validation, Data Curation. **Haibing Shao:** Methodology, Software, Writing - Review & Editing, Resources, Supervision.

Declaration of competing interest

The authors declare that they have no known competing financial interests or personal relationships that could have appeared to influence the work reported in this paper.

Acknowledgements

This research is financially supported by the Key Research and Development Project of Shaanxi Province (2020ZDLSF06-08), as well as the Open

Project of Key Laboratory of Coal Resources Exploration and Comprehensive Utilization (KF2020-7, KF2021-1), which is funded by the Chinese Ministry of Natural Resources.

References

[1] N. Kittner, F. Lill, D. M. Kammen, Energy storage deployment and innovation for the clean energy transition, Nature Energy 2 (2017) 1–6.

[2] N. Zhao, F. You, Can renewable generation, energy storage and energy efficient technologies enable carbon neutral energy transition?, Applied Energy 279 (2020) 115889.

[3] Z. Jia, B. Lin, How to achieve the first step of the carbon-neutrality 2060 target in china: the coal substitution perspective, Energy (2021) 121179.

[4] J. W. Lund, A. N. Toth, Direct utilization of geothermal energy 2020 worldwide review, Geothermics (2020) 101915.

[5] A. Anderson, B. Rezaie, Geothermal technology: Trends and potential role in a sustainable future, Applied Energy 248 (2019) 18–34.

[6] D. Ürge-Vorsatz, L. F. Cabeza, S. Serrano, C. Barreneche, K. Petrichenko, Heating and cooling energy trends and drivers in buildings, Renewable and Sustainable Energy Reviews 41 (2015) 85–98.

[7] J. Lin, B. Lin, The actual heating energy conservation in china: Evidence and policy implications, Energy and Buildings 190 (2019) 195–201.

[8] J. M. Dias, V. A. Costa, Adsorption heat pumps for heating applications: A review of current state, literature gaps and development challenges, Renewable and Sustainable Energy Reviews 98 (2018) 317–327.

[9] M. Soltani, F. M. Kashkooli, A. Dehghani-Sanij, A. Kazemi, N. Bordbar, M. Farshchi, M. Elmi, K. Gharali, M. B. Dusseault, A comprehensive study of geothermal heating and cooling systems, Sustainable Cities and Society 44 (2019) 793–818.

[10] H. Javadi, S. S. M. Ajarostaghi, M. A. Rosen, M. Pourfallah, Performance of ground heat exchangers: A comprehensive review of recent advances, Energy 178 (2019) 207–233.

[11] L. Xu, L. Pu, S. Zhang, Y. Li, Hybrid ground source heat pump system for overcoming soil thermal imbalance: A review, Sustainable Energy Technologies and Assessments 44 (2021) 101098.

[12] T. Kohl, R. Brenni, W. Eugster, System performance of a deep borehole heat exchanger, Geothermics 31 (2002) 687–708.

[13] K. Morita, W. S. Bollmeier, H. Mizogami, An experiment to prove the concept of the downhole coaxial heat exchanger (dche) in hawaii, Geothermal Resources Council (1992).

[14] T. Kohl, M. Salton, L. Rybach, Data analysis of the deep borehole heat exchanger plant weissbad (switzerland), in: Proceedings world geothermal congress, 2000, pp. 3459–3464.

[15] T. Śliwa, J. Kotyza, Application of existing wells as ground heat source for heat pumps in poland, Applied Energy 74 (2003) 3–8.

[16] T. Kujawa, W. Nowak, A. A. Stachel, Utilization of existing deep geological wells for acquisitions of geothermal energy, Thermal Sciences 2004. Proceedings of the ASME-ZSIS International Thermal Science Seminar II (2004).

[17] A. Sapinska-Sliwa, M. A. Rosen, A. Gonet, T. Sliwa, Deep borehole heat exchangers—a conceptual and comparative review, International Journal of Air-Conditioning and Refrigeration 24 (2016) 1630001.

[18] Z. Wang, F. Wang, J. Liu, Z. Ma, E. Han, M. Song, Field test and numerical investigation on the heat transfer characteristics and optimal design of the heat exchangers of a deep borehole ground source heat pump system, Energy Conversion and Management 153 (2017) 603–615.

[19] J. Deng, Q. Wei, M. Liang, S. He, H. Zhang, Field test on energy performance of medium-depth geothermal heat pump systems (md-ghps), Energy and Buildings 184 (2019) 289–299.

[20] Y. Huang, Y. Zhang, Y. Xie, Y. Zhang, X. Gao, J. Ma, Field test and numerical investigation on deep coaxial borehole heat exchanger based on distributed optical fiber temperature sensor, Energy 210 (2020) 118643.

[21] J. Deng, S. He, Q. Wei, J. Li, H. Liu, Z. Zhang, H. Zhang, Field test and optimization of heat pumps and water distribution systems in medium-depth geothermal heat pump systems, Energy and Buildings 209 (2020) 109724.

[22] A. Pan, L. Lu, P. Cui, L. Jia, A new analytical heat transfer model for deep borehole heat exchangers with coaxial tubes, International Journal of Heat and Mass Transfer 141 (2019) 1056–1065.

[23] Y. Luo, H. Guo, F. Meggers, L. Zhang, Deep coaxial borehole heat exchanger: Analytical modeling and thermal analysis, Energy 185 (2019) 1298–1313.

[24] X. Song, G. Wang, Y. Shi, R. Li, Z. Xu, R. Zheng, Y. Wang, J. Li, Numerical analysis of heat extraction performance of a deep coaxial borehole heat exchanger geothermal system, Energy 164 (2018) 1298–1310.

[25] L. Fang, N. Diao, Z. Shao, K. Zhu, Z. Fang, A computationally efficient numerical model for heat transfer simulation of deep borehole heat exchangers, Energy and Buildings 167 (2018) 79–88.

[26] M. Le Lous, F. Larroque, A. Dupuy, A. Moignard, Thermal performance of a deep borehole heat exchanger: Insights from a synthetic coupled heat and flow model, Geothermics 57 (2015) 157–172.

[27] C. Li, Y. Guan, J. Liu, C. Jiang, R. Yang, X. Hou, Heat transfer performance of a deep ground heat exchanger for building heating in long-term service, Renewable Energy 166 (2020) 20–34.

[28] X. Hu, J. Banks, L. Wu, W. V. Liu, Numerical modeling of a coaxial borehole heat exchanger to exploit geothermal energy from abandoned petroleum wells in hinton, alberta, Renewable Energy 148 (2020) 1110–1123.

[29] Y. Kong, C. Chen, H. Shao, P. Zhonghe, X. Liangping, W. Jiyang, Principle and capacity quantification of deep-borehole heat exchangers, Chinese journal of geophysics 60 (2017) 4741–4752.

[30] R. A. Beier, Thermal response tests on deep borehole heat exchangers with geothermal gradient, Applied Thermal Engineering (2020) 115447.

[31] J. Liu, F. Wang, W. Cai, Z. Wang, C. Li, Numerical investigation on the effects of geological parameters and layered subsurface on the thermal performance of medium-deep borehole heat exchanger, Renewable Energy 149 (2020) 384–399.

[32] W. Cai, F. Wang, J. Liu, Z. Wang, Z. Ma, Experimental and numerical investigation of heat transfer performance and sustainability of deep borehole heat exchangers coupled with ground source heat pump systems, Applied Thermal Engineering (2018).

[33] T. Xu, Z. Hu, B. Feng, G. Feng, F. Li, Z. Jiang, Numerical evaluation of building heating potential from a co-axial closed-loop geothermal system using wellbore–reservoir coupling numerical model, Energy Exploration & Exploitation 38 (2020) 733–754.

[34] J. Liu, F. Wang, Y. Gao, Y. Zhang, W. Cai, M. Wang, Z. Wang, Influencing factors analysis and operation optimization for the long-term performance of medium-deep borehole heat exchanger coupled ground source heat pump system, Energy and Buildings 226 (2020) 110385.

[35] S. Lazzari, A. Priarone, E. Zanchini, Long-term performance of bhe (borehole heat exchanger) fields with negligible groundwater movement, Energy 35 (2010) 4966–4974.

[36] A. Gultekin, M. Aydin, A. Sisman, Thermal performance analysis of multiple borehole heat exchangers, Energy Conversion and Management 122 (2016) 544–551.

[37] S. Chen, F. Witte, O. Kolditz, H. Shao, Shifted thermal extraction rates in large borehole heat exchanger array–a numerical experiment, Applied Thermal Engineering 167 (2020) 114750.

[38] P. Bayer, M. de Paly, M. Beck, Strategic optimization of borehole heat exchanger field for seasonal geothermal heating and cooling, Applied energy 136 (2014) 445–453.

[39] O. Ozgener, L. Ozgener, J. W. Tester, A practical approach to predict soil temperature variations for geothermal (ground) heat exchangers applications, International Journal of Heat and Mass Transfer 62 (2013) 473–480.

[40] D. Yener, O. Ozgener, L. Ozgener, Prediction of soil temperatures for shallow geothermal applications in turkey, Renewable and Sustainable Energy Reviews 70 (2017) 71–77.

[41] W. Cai, F. Wang, S. Chen, C. Chen, J. Liu, J. Deng, O. Kolditz, H. Shao, Analysis of heat extraction performance and long-term sus-

tainability for multiple deep borehole heat exchanger array: A project-based study, Applied Energy 289 (2021) 116590.

[42] X. Bu, K. Jiang, H. Li, Performance of geothermal single well for intermittent heating, Energy 186 (2019) 115858.

[43] C. Chen, H. Shao, D. Naumov, Y. Kong, K. Tu, O. Kolditz, Numerical investigation on the performance, sustainability, and efficiency of the deep borehole heat exchanger system for building heating, Geothermal Energy 7 (2019) 18.

[44] H.-J. Diersch, D. Bauer, W. Heidemann, W. Rühaak, P. Schätzl, Finite element modeling of borehole heat exchanger systems: Part 1. fundamentals, Computers & Geosciences 37 (2011) 1122–1135. doi:10.1016/j.cageo.2010.08.003.

[45] H. Shao, P. Hein, A. Sachse, O. Kolditz, Geoenergy Modeling II: Shallow Geothermal Systems, Springer, 2016.

[46] O. Kolditz, S. Bauer, L. Bilke, N. Böttcher, J.-O. Delfs, T. Fischer, U. J. Görke, T. Kalbacher, G. Kosakowski, C. McDermott, et al., Opengeosys: an open-source initiative for numerical simulation of thermo-hydro-mechanical/chemical (thm/c) processes in porous media, Environmental Earth Sciences 67 (2012) 589–599.

[47] R. Al-Khoury, T. Kölbel, R. Schramedei, Efficient numerical modeling of borehole heat exchangers, Computers & Geosciences 36 (2010) 1301–1315.

[48] H.-J. Diersch, D. Bauer, W. Heidemann, W. Rühaak, P. Schätzl, Finite element modeling of borehole heat exchanger systems: Part 2. numerical simulation, Computers & Geosciences 37 (2011) 1136–1147. doi:10.1016/j.cageo.2010.08.002.

[49] L. Bilke, H. Shao, S. Chen, W. Cai, OpenGeoSys Tutorial, Website, 2020. https://www.opengeosys.org/docs/userguide/basics/introduction/.

[50] F. Witte, I. Tuschy, Tespy: Thermal engineering systems in python, Journal of Open Source Software 5 (2020) 2178.

[51] C. Chen, W. Cai, D. Naumov, K. Tu, H. Zhou, Y. Zhang, O. Kolditz, H. Shao, Numerical investigation on the capacity and efficiency of

a deep enhanced u-tube borehole heat exchanger system for building heating, Renewable Energy 169 (2021) 557–572.

[52] B. Meng, T. Vienken, O. Kolditz, H. Shao, Evaluating the thermal impacts and sustainability of intensive shallow geothermal utilization on a neighborhood scale: Lessons learned from a case study, Energy Conversion and Management 199 (2019) 111913.

[53] S. Chen, W. Cai, F. Witte, X. Wang, F. Wang, O. Kolditz, et al, Long-term thermal imbalance in large borehole heat exchangers array-a numerical study based on the leicester project, Energy and Buildings (2020) 110518.

[54] R. Song, J. Guang-Zheng, G. Ya-Jie, H. Sheng-Biao, W. Ji-Yang, The thermal structure of the lithosphere and heat source mechanism of geothermal field in weihe basin, Chinese Journal of Geophysics-Chinese edition 59 (2016) 2176–2190.

[55] Z. Ren, R. Liu, W. Ren, K. Qi, G. Yang, J. Cui, P. Yang, Y. Zhang, Distribution of geothermal field and its controlling factors in the weihe basin, ACTA GEOLOGICA SINICA 94 (2020) 1938–1949.

[56] S. Chen, Q. Zhang, H. Li, B. Mclellan, T. Zhang, Z. Tan, Investment decision on shallow geothermal heating & cooling based on compound options model: A case study of china, Applied Energy 254 (2019) 113655.